Phase conjugation in liquid suspensions of microspheres in the diffusive limit

D. Rogovin and S. O. Sari
Rockwell International, Science Center, 1049 Camino Dos Rios, Thousand Oaks, California 91360
(Received 25 October 1984)

We examine phase conjugation via degenerate four-wave mixing in liquid suspensions of microspheres in the small-field limit, where saturation effects can be ignored. For these media, electrostrictive forces modulate the microparticle density in such a way that two orthogonal spatial gratings are created. Coherent scattering of the pump radiation from these two gratings gives rise to the formation of a conjugate wave, as well as amplification of the probe wave. We discuss the steady-state and transient characteristics of the probe and conjugate waves in this regime where the dynamics of the microparticles is governed by diffusion.

I. INTRODUCTION

Phase conjugation has recently attracted considerable interest in the nonlinear-optics community.[1–3] Numerous fundamental and applied investigations have underscored the scientific significance and potential device applications of this class of phenomena. For example, phase conjugation has been observed in a variety of atomic[4] and molecular gases,[5] several liquids,[6] and a large number of solids.[7] Furthermore, various approaches to phase conjugation, i.e., degenerate four-wave mixing,[8] three-wave mixing,[9] and stimulated scattering[10] have been extensively examined in steady-state, and for some cases, transient situations.[11] Finally, numerous theoretical and experimental investigations regarding device applications of phase conjugation in the fields of aberration compensation,[12] photolithography,[13] and spatial information processing[14] have been undertaken.

One class of media which we find particularly interesting, and which is the subject of this paper, is artificial dielectrics; in particular, liquid[15] and gaseous suspensions[16] of microparticles. For these media, nonlinear optical phenomena arise from a variety of electrostrictive mechanisms[17] which may alter the density, orientation,[18] size or shape of the microparticles. In turn, these alterations give rise to changes in the index of refraction of the suspension and, hence, to nonlinear optical effects such as phase conjugation. For example, if a liquid suspension of nonabsorbing microspheres is irradiated with laser light, electrostrictive forces will modulate the particulate density. So long as the index of refraction of the microparticles differs from that of the host fluid, the refractive index of the entire suspension will be spatially modulated by the laser radiation. Furthermore, because the particulates are nearly macroscopic in size, i.e., on the order of several hundred to several thousand angstroms, they are extremely polarizable, and this gives rise to unusually large nonlinear optical coefficients. In addition, such media will be relatively slow in comparison to typical atomic media, since nonlinear effects arise from the redistribution of the particulate density in a viscous medium. Note, too, that for these media, resonant processes are not usually expected to play a significant role in the generation of conjugate waves.

Recently, Smith *et al.*[15] have reported some very interesting experimental work in which they observed degenerate four-wave mixing in a medium composed of a liquid suspension of microparticles. In their experiments, they measured the efficiency and response time for the production of conjugate waves by an aqueous suspension of 1000-Å latex spheres irradiated by an Ar^+ laser emitting on the 0.5145-μm line. This paper has been motivated, in part, by these developments. Thus, our interest is to give a theoretical formulation of phase conjugation via degenerate four-wave mixing in a liquid suspension of microspheres whose size is small compared to the radiation wavelength. We discuss the steady-state and transient characteristics of both the conjugate and probe waves in the nondepleted pump approximation. We assume that the electrostrictive forces are sufficiently weak that only a small fraction of the microparticles are involved in four-wave mixing, so that there are no saturation effects. This implies that if U denotes the electrostrictive potential and T the temperature, then we consider only effects of order U/kT in the microparticle density. Note that we are not necessarily limited to the small-signal regime with regard to the conjugate wave, since within the same approximation, it is still possible to have

$$\kappa L \sim 1 , \tag{1.1}$$

where κ is the four-wave-mixing coefficient and L is the interaction length.

In Sec. II we develop the fundamental equations which describe degenerate four-wave mixing in liquid suspensions of microspheres. Section III is devoted to the steady-state case where we discuss the polarization and efficiency of both the conjugate and probe waves. Time-dependent situations are discussed in Sec. IV. In particular, we examine the transient behavior of the medium as it is driven from one state to another by electromagnetic radiation. More precisely, we study the evolution to a steady state from the initial thermal equilibrium state of a uniform microparticle density. Finally, in Sec. V we summarize our results and discuss our conclusions.

II. FORMULATION

For convenience, we consider a liquid suspension of identical, nonabsorbing microspheres of radius a, which

are irradiated by three external laser beams of frequency ω: two counterpropagating pump waves and a probe wave, as depicted in Fig. 1. If $\mathbf{E}(\mathbf{r},t)$ denotes the total radiation field, the microparticles will each feel an electrostrictive force $\mathbf{F}(\mathbf{r},t)$ given by[16,17]

$$\mathbf{F}(\mathbf{r},t)=\tfrac{1}{2}\alpha(\omega)\nabla\bar{E}^{2}(\mathbf{r},t)\ , \tag{2.1}$$

where the overbar implies a time average over many optical periods and the radiation wavelength $\lambda \gg a$. In Eq. (2.1), the quantity $\alpha(\omega)$ is the polarizability at the laser frequency which is given by

$$\alpha(\omega)=\epsilon_h(\omega)\left[\frac{\epsilon_r(\omega)-1}{\epsilon_r(\omega)+2}\right]a^3\ . \tag{2.2}$$

Here, $\epsilon_h(\omega)$ is the frequency-dependent dielectric constant of the host liquid and $\epsilon_r(\omega)$ is the ratio of the dielectric constant of the microparticle to $\epsilon_h(\omega)$. Since $\nabla\times\mathbf{F}(\mathbf{r},t)=\mathbf{0}$, it follows that the microparticles are immersed in an electrostrictive potential $U(\mathbf{r},t)$ given by

$$U(\mathbf{r},t)=-\tfrac{1}{2}\alpha(\omega)\bar{E}^{2}(\mathbf{r},t)\ , \tag{2.3}$$

and consequently will tend to move to regions where $U(\mathbf{r},t)$ is smallest. If $\epsilon_r>1$, this corresponds to regions where the field intensity is greatest; whereas if $\epsilon_r<1$, this corresponds to regions where the field intensity is at a minimum. Thus, the microparticle density $n(\mathbf{r},t)$ will be modulated by electrostrictive forces, and we now consider techniques for calculating $n(\mathbf{r},t)$.

Since the microparticles are suspended in a liquid, diffusion assumes an important role in their dynamics. Accordingly, we begin with the Chandrasekhar equation[19] for the distribution function $f(\mathbf{r},\mathbf{u};t)$

$$\frac{\partial f}{\partial t}=\mathbf{u}\cdot\nabla_r f+\frac{1}{m}\mathbf{F}\cdot\nabla_u f+\beta\left[\nabla_u\cdot(f\mathbf{u})+\frac{kT}{m}\nabla_u^2 f\right]\ , \tag{2.4}$$

where $\mathbf{r}(\mathbf{u})$ denotes the microparticle position (velocity) and ∇_r (∇_u) is the corresponding vector derivative operator. The coefficient β is defined by

$$\beta=6\pi\nu a/m\ , \tag{2.5}$$

where ν is the viscosity of the liquid, m the mass of the microparticles, and T the temperature.

Before proceeding, it is worth commenting on the physical content of Eq. (2.4). The first two terms on the right-hand side of the Chandrasekhar equation are identical to the corresponding terms that appear in the Boltzmann equation. However, in place of the collision term that appears in the Boltzmann equation[20]

$$\left[\frac{\partial f}{\partial t}\right]_c=\frac{f-f_0}{\tau_c}\ , \tag{2.6}$$

where f_0 is the equilibrium distribution and τ_c the collisional relaxation time, the Chandrasekhar equation has the terms

$$\beta[\nabla_u\cdot(f\mathbf{u})+(kT/m)\nabla_u^2 f]$$

which represent relaxation of the velocity distribution due to diffusion processes. Note that in thermodynamic equilibrium with $\mathbf{F}=\mathbf{0}$, $f=f(u)$ only and Eq. (2.4) becomes

$$\beta[\nabla_u\cdot(\mathbf{u}f)+(kT/m)\nabla_u^2 f]=0\ . \tag{2.7}$$

The solution of Eq. (2.7) is the well-known Maxwell-Boltzmann distribution function,

$$f(u)=\left[\frac{m}{2\pi kT}\right]^{3/2}\exp\left[-\frac{mu^2}{2kT}\right]\ . \tag{2.8}$$

For our purposes, we do not require detailed information regarding the microparticle velocity distribution. In particular, the polarization of the medium is determined by the microparticle density

$$n(\mathbf{r},t)=\int d^3u\, f(\mathbf{r},\mathbf{u};t)\ . \tag{2.9}$$

Consequently, we should like to extract a dynamic equation for the microparticle density from the Chandrasekhar equation. To do so, it is necessary to make some assumption regarding the behavior of the microparticle velocity distribution. On physical grounds, we anticipate that the velocity of the microparticles should approach equilibrium with the surrounding host fluid regardless of the state of the microparticle density. This arises because the velocity distribution of the microparticles is governed by collisions with the fluid molecules and therefore should relax rapidly to thermodynamic equilibrium. To estimate the space and time scales over which this happens, we note that from the coefficients β and kT/m, one can construct the following temporal and spatial scales:

$$\tau=1/\beta=\frac{m}{6\pi\nu a}\ , \tag{2.10a}$$

$$l=\left[\frac{kT}{m}\right]^{1/2}\frac{1}{\beta}\simeq\bar{u}\tau\ , \tag{2.10b}$$

where $\bar{u}$ is the thermal velocity. These scales should govern the basic times and lengths over which the microparticle velocity distribution will relax. If $\mathbf{F}(\mathbf{r},t)$ varies slowly over these scales and for times long compared to τ, we can assume that the microparticle velocity distribution is near thermodynamic equilibrium with the surrounding fluid (which is maintained at a temperature T). Thus, we take the distribution to be slowly perturbed only in the space and time coordinates and write

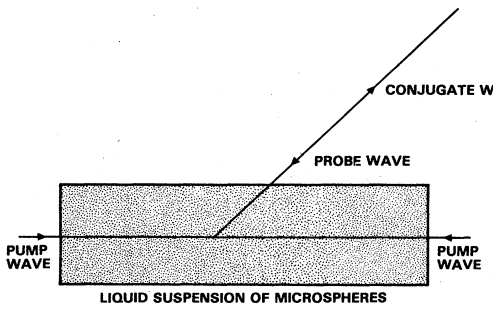

FIG. 1. Basic geometry of phase conjugation via degenerate four-wave mixing.

$$f(\mathbf{r},\mathbf{u};t)=\left[\frac{m}{2\pi kT}\right]^{3/2} e^{-mu^2/2kT} n(\mathbf{r},t) . \tag{2.11}$$

Inserting Eq. (2.11) into the Chandrasekhar equation, we obtain

$$\frac{\partial n}{\partial t}=D\nabla\cdot\left[\nabla n(\mathbf{r},t)-\frac{\mathbf{F}(\mathbf{r},t)}{kT}n(\mathbf{r},t)\right] , \tag{2.12}$$

where D is the diffusion coefficient for microspheres in a liquid, i.e.,

$$D=\frac{kT}{6\pi\nu a} . \tag{2.13}$$

Equation (2.12) is the Planck-Nernst equation for the microparticle density and the quantity in the large parentheses times the diffusion coefficient is the microparticle flux $\mathbf{J}(\mathbf{r},t)$.

Finally, we evaluate the magnitude of τ and l and thereby obtain an estimate of the space and time scales over which the Planck-Nernst equation is valid. As a specific case in point, we consider 1000-Å latex microspheres suspended in water at room temperature. For this system, the microparticle mass density is on the order of 1 g/cm^3 and

$$\tau\simeq 2\times 10^{-9}\text{ s} ,$$

$$l\simeq 6\times 10^{-10}\text{ cm} .$$

For our purposes, we shall be concerned with time scales no shorter than microseconds and length scales which are greater than a few tenths of a micrometer, so that Eq. (2.12) should be suitable.

III. STEADY-STATE CHARACTERISTICS

In this section we examine the steady-state characteristics of the conjugate wave generated via electrostrictive forces acting on a liquid suspension of nonabsorbing microspheres. Consequently, we require the nonlinear polarization $\mathbf{P}_{\mathrm{NL}}^{(c)}(\mathbf{r},t)$ that is associated with phase conjugation. We can calculate this quantity by first noting that the total polarization vector for a suspension of identical microparticles in an electromagnetic field $\mathbf{E}(\mathbf{r},t)$ is

$$\mathbf{P}(\mathbf{r},t)=\alpha(\omega)n(\mathbf{r})\mathbf{E}(\mathbf{r},t) . \tag{3.1}$$

In Eq. (3.1), $n(\mathbf{r})$ is the steady-state solution of Eq. (2.12) which is

$$n(r)=N\frac{e^{-U(\mathbf{r})/kT}}{\int d^3r\, e^{-U(\mathbf{r})/kT}} , \tag{3.2}$$

where N is the total number of microparticles and $U(\mathbf{r})$ is given by Eq. (2.3). In the weak-field limit, where the electrostrictive potential is small compared to kT, one can expand in powers of U/kT, and Eq. (3.4) reduces to

$$n(\mathbf{r})=n_0\left[1-\left[\frac{U(\mathbf{r})}{kT}-\frac{\langle U(\mathbf{r})\rangle}{kT}\right]\right] , \tag{3.3}$$

where the angular brackets imply a spatial average over the volume containing the microparticles and n_0 is the microparticle density in the absence of electrostrictive forces. Inserting Eq. (3.3) into Eq. (3.1), using Eq. (2.3), and extracting the third-order polarization, we have

$$\mathbf{P}_{\mathrm{NL}}^{(3)}(\mathbf{r},t)=n_0\frac{\alpha^2(\omega)}{2kT}[\overline{E^2(\mathbf{r},t)}-\langle\overline{E^2(\mathbf{r},t)}\rangle]\mathbf{E}(\mathbf{r},t) . \tag{3.4}$$

To make further progress, we must specify $\mathbf{E}(\mathbf{r},t)$. If we neglect the contribution due to Rayleigh scattering,

$$\mathbf{E}(\mathbf{r},t)=\sum_{j=1,2,p,c}\epsilon_j(\mathbf{r})\hat{e}_j e^{i(\omega_j t-\mathbf{k}_j\cdot\mathbf{r})}+\text{c.c.} , \tag{3.5}$$

where $j=1,2$ refers to the counterpropagating pump beams, $j=p$ the probe wave, and $j=c$ the conjugate wave. The quantities $\epsilon_j(\mathbf{r})$ are the complex field amplitudes, $\hat{e}_j$ the normalized polarization vectors, ω_j the laser frequencies, and $\mathbf{k}_j$ the corresponding wave vectors. In the fully degenerate case,

$$\omega_j=\omega \quad \text{for } j=1,2,p,c , \tag{3.6a}$$

$$\mathbf{k}_1=-\mathbf{k}_2\equiv\mathbf{K} , \tag{3.6b}$$

$$\mathbf{k}_p=-\mathbf{k}_c=\mathbf{Q} . \tag{3.6c}$$

Now, the probe and conjugate waves vary as $e^{i(\omega t\pm\mathbf{Q}\cdot\mathbf{r})}$, and it follows that only those terms in Eq. (3.4) with the same phasors will contribute to the production of a conjugate wave. Collecting these terms, we find for the component of a third-order polarization of interest, $\mathbf{P}_{\mathrm{NL}}^{(c)}(\mathbf{r},t)$,

$$\begin{aligned}\mathbf{P}_{\mathrm{NL}}^{(c)}(\mathbf{r},t)=&\left[n_0\frac{\alpha^2(\omega)}{2kT}E_1E_2E_p^*[(\hat{e}_p^*\cdot\hat{e}_1)\hat{e}_2+(\hat{e}_p^*\cdot\hat{e}_2)\hat{e}_1]e^{i(\omega t+\mathbf{Q}\cdot\mathbf{r})}+\text{c.c.}\right]\\&-\left[n_0\frac{\alpha^2(\omega)}{2kT}E_1E_2E_c[(\hat{e}_c^*\cdot\hat{e}_1)\hat{e}_2+(\hat{e}_c^*\cdot\hat{e}_2)\hat{e}_1]e^{i(\omega t-\mathbf{Q}\cdot\mathbf{r})}+\text{c.c.}\right]\\&-\left[n_0\frac{\alpha^2(\omega)}{2kT}E_c[E_1^2(\hat{e}_1^*\cdot\hat{e}_c)\hat{e}_1+E_2^2(\hat{e}_2^*\cdot\hat{e}_c)\hat{e}_2]e^{i(\omega t-\mathbf{Q}\cdot\mathbf{r})}+\text{c.c.}\right]\\&-\left[n_0\frac{\alpha^2(\omega)}{2kT}E_p[E_1^2(\hat{e}_1^*\cdot\hat{e}_p)\hat{e}_1+E_2^2(\hat{e}_2^*\cdot\hat{e}_s)\hat{e}_2]e^{i(\omega t+\mathbf{Q}\cdot\mathbf{r})}+\text{c.c.}\right] ,\end{aligned} \tag{3.7}$$

where we have ignored the phase of the pump waves. The last two terms in Eq. (3.7) affect only the phases of the conjugate and probe waves as they propagate through the nonlinear medium. Accordingly, interest focuses on the first and second terms which can be written in the following form:

$$-n_0\frac{\alpha^2(\omega)}{2kT}[(\overline{\mathbf{E}_1\cdot\mathbf{E}_s^*})\mathbf{E}_2+(\overline{\mathbf{E}_2\cdot\mathbf{E}_s^*})\mathbf{E}_1]$$

$$-n_0\frac{\alpha^2(\omega)}{2kT}[(\overline{\mathbf{E}_1\cdot\mathbf{E}_c^*})\mathbf{E}_2+(\overline{\mathbf{E}_2\cdot\mathbf{E}_c^*})\mathbf{E}_2]\ ,$$

where the overbars imply a time average over several optical periods. Note that no terms of the form

$$-n_0\frac{\alpha^2(\omega)}{2kT}[(\overline{\mathbf{E}_1\cdot\mathbf{E}_2})\mathbf{E}_s^*+(\overline{\mathbf{E}_1\cdot\mathbf{E}_2})\mathbf{E}_c^*]$$

have been included. At first glance, this might appear somewhat unusual as terms of this form, without the time average, generally appear as two-photon resonances in atomic, molecular, or solid-state media in which conjugate waves are generated via virtual transitions to various quantum states. To see why, we note that

$$\mathbf{E}_1\cdot\mathbf{E}_2=2E_1E_2\,\mathrm{Re}[(\hat{e}_1\cdot\hat{e}_2)e^{2i\mathbf{K}\cdot\mathbf{r}}+(\hat{e}_1\cdot\hat{e}_2)e^{2i\omega t}]\ . \tag{3.8}$$

If we now construct $(\mathbf{E}_1\cdot\mathbf{E}_2)\mathbf{E}_s^*$, we find that only the second term in Eq. (3.8) gives rise to a conjugate wave. However, the microparticles cannot respond to this force as it oscillates at an optical frequency and therefore will vanish upon time averaging. Consequently, no term of the form $(\mathbf{E}_1\cdot\mathbf{E}_2)\mathbf{E}_s^*$ appears in the nonlinear polarization for a medium composed of a suspension of microparticles.

To obtain a more detailed understanding of the physical content of Eq. (3.7), we construct the perturbed microparticle distribution, $\delta n(\mathbf{r})$ that generates conjugate waves. In particular, the microparticle distribution is perturbed by electrostrictive forces in such a way that two different spatial gratings, with periods $\Lambda_\pm\equiv 2\pi/|\mathbf{K}\pm\mathbf{Q}|$, are formed. Since $K=Q$, these two spatial gratings are orthogonal to each other and we can write the perturbed microparticle distribution as

$$\delta n(x,y)=-n_0\frac{\alpha(\omega)}{2kT}\,\mathrm{Re}[\,E_1E_p^*(\hat{e}_1\cdot\hat{e}_p^*)\exp(2\pi ix/\Lambda_-)+E_2E_p^*(\hat{e}_2\cdot\hat{e}_p^*)\exp(-2\pi iy/\Lambda_+)$$
$$+E_1E_c^*(\hat{e}_1\cdot\hat{e}_c^*)\exp(2\pi iy/\Lambda_+)+E_2E_c^*(\hat{e}_2\hat{e}_c^*)\exp(-2\pi ix/\Lambda_-)]\ . \tag{3.9}$$

Here, x and y are coordinates along the directions defined by $\mathbf{K}-\mathbf{Q}$ and $\mathbf{K}+\mathbf{Q}$, and

$$\Lambda_+(\theta)\equiv\frac{\lambda}{2\cos(\theta/2)}\ , \tag{3.10a}$$

$$\Lambda_-(\theta)\equiv\frac{\lambda}{2\sin(\theta/2)} \tag{3.10b}$$

with θ the angle between $\mathbf{K}$ and $\mathbf{Q}$.

Next, we construct the equation for the propagation of probe and conjugate waves in steady-state situations. We begin with the Maxwell equations and following the usual procedure, we have

$$\left[\nabla^2-\frac{1}{c^2}\frac{\partial^2}{\partial t^2}\right]\mathbf{E}(\mathbf{r},t)=\frac{4\pi}{c^2}\frac{\partial^2\mathbf{P}}{\partial t^2}\ , \tag{3.11}$$

where the polarization $\mathbf{P}(\mathbf{r},t)$ contains a linear as well as a nonlinear piece. The linear term describes Rayleigh scattering due to the presence of the microparticles, as well as the fact that the speed of light in the medium is v. If we approximate the scattering contribution as a simple loss, we have

$$\left[\nabla^2-\frac{1}{v^2}\frac{\partial^2}{\partial t^2}-\frac{4\pi i}{c^2}\chi''\frac{\partial^2}{\partial t^2}\right]\mathbf{E}(\mathbf{r},t)=\frac{4\pi}{c^2}\frac{\partial^2}{\partial t^2}\mathbf{P}_{\mathrm{NL}}\ , \tag{3.12}$$

where $\chi''=\frac{1}{2}L_s^{-1}$ and $L_s^{-1}=8\pi/3a^2n_0(2\pi a/\lambda)^4$ is the extinction coefficient.[21] Note that this approach does not treat multiple scattering and therefore is valid only for dilute media. Next, we insert Eqs. (3.5)–(3.7) into Eq. (3.12) and we obtain

$$(2i\mathbf{Q}\cdot\nabla+i\alpha Q)\epsilon_c(\mathbf{r},t)\hat{e}_c=-n_0\alpha(\omega)Q^2\frac{\alpha(\omega)E_1E_2}{2kT}[(\hat{e}_p^*\cdot\hat{e}_1)\hat{e}_2+(\hat{e}_p^*\cdot\hat{e}_2)\hat{e}_1]\epsilon_p^*(\hat{r},t)$$
$$-n_0\alpha(\omega)\frac{\alpha(\omega)E_1E_2}{2kT}Q^2\left[\frac{E_1}{E_2}(\hat{e}_1^*\cdot\hat{e}_c)\hat{e}_1+\frac{E_2}{E_1}(\hat{e}_2^*\cdot\hat{e}_c)\hat{e}_2\right]\epsilon_c(\mathbf{r},t)\ , \tag{3.13a}$$

$$(-2i\mathbf{Q}\cdot\nabla+i\alpha Q)\epsilon_p(\mathbf{r},t)\hat{e}_p=-n_0\alpha(\omega)Q^2\frac{\alpha(\omega)E_1E_2}{2kT}[(\hat{e}_c^*\cdot\hat{e}_1)\hat{e}_2+(\hat{e}_c^*\cdot\hat{e}_2)\hat{e}_1]\epsilon_c^*(\mathbf{r},t)$$
$$-n_0\alpha(\omega)\frac{\alpha(\omega)E_1E_2}{2kT}Q^2[(E_1/E_2)(\hat{e}_1^*\cdot\hat{e}_p)\hat{e}_1+(E_2/E_1)(\hat{e}_2^*\cdot\hat{e}_p)\hat{e}_2]\epsilon_p(\mathbf{r},t)\ . \tag{3.13b}$$

Equations (3.13) are first-order coupled vector differential equations for the polarization vectors and complex amplitudes of the probe and conjugate waves. To obtain a greater appreciation of the physical content of these equations, we first consider the case in which there are no scattering losses and the pump amplitudes, which we denote by E, are equal. Then,

$$\left[\frac{d}{dz}-i\kappa\right]\epsilon_c(z)\hat{e}_c=i\kappa[(\hat{e}_p\cdot\hat{e}_1)\hat{e}_2+(\hat{e}_p^*\cdot\hat{e}_2)\hat{e}_1]\epsilon_p^*(z)\ , \tag{3.14a}$$

$$\left[\frac{d}{dz}-i\kappa\right]\epsilon_p^*(z)\hat{e}_p=i\kappa[(\hat{e}_c^*\cdot\hat{e}_1)\hat{e}_2+(\hat{e}_c^*\cdot\hat{e}_2)\hat{e}_1]\epsilon_c(z)\ , \tag{3.14b}$$

where

$$\kappa=\tfrac{1}{4}n_0\alpha(\omega)Q\frac{\alpha(\omega)E^2}{kT} . \tag{3.15}$$

The second term on the left-hand side of Eqs. (3.14) alters the phase, but not the amplitudes of the probe and conjugate waves. Accordingly, we set[22]

$$\epsilon_c(z)=\tilde{\epsilon}_c(z)e^{-i\kappa z} , \tag{3.16a}$$

$$\epsilon_p(z)=\tilde{\epsilon}_p(z)e^{i\kappa z} , \tag{3.16b}$$

and will confine ourselves to $\tilde{\epsilon}_c(z)$ and $\tilde{\epsilon}_p(z)$. To solve Eqs. (3.14), it is convenient to introduce two orthonormal vectors, $\hat{a}_1$ and $\hat{a}_2$, defined by

$$\hat{a}_1\equiv\frac{1}{\sqrt{2}}(\hat{e}_1+\hat{e}_2) , \tag{3.17a}$$

$$\hat{a}_2\equiv\frac{1}{\sqrt{2}}(\hat{e}_1-\hat{e}_2) . \tag{3.17b}$$

Then

$$\hat{e}_c\equiv\frac{(\hat{e}_p^*\cdot\hat{a}_1)\hat{a}_1-(\hat{e}_p^*\cdot\hat{a}_2)\hat{a}_2}{(|\hat{e}_p^*\cdot\hat{a}_1|^2+\hat{e}_p^*\cdot\hat{a}_2|^2)^{1/2}} \tag{3.18}$$

and Eqs. (3.13) reduce to the standard form

$$\frac{d^2}{dz^2}\tilde{\epsilon}_c=-\tilde{\kappa}^2\tilde{\epsilon}_c , \tag{3.19a}$$

$$\frac{d^2}{dz^2}\tilde{\epsilon}_p^*=-\tilde{\kappa}^2\tilde{\epsilon}_p^* , \tag{3.19b}$$

where

$$\tilde{\kappa}\equiv\kappa[|\hat{e}_p^*\cdot\hat{a}_1|^2+|\hat{e}_p^*\cdot\hat{a}_2|^2]^{1/2} . \tag{3.20}$$

It is worth noting that despite the fact that we have treated the electrostrictive interactions only to first order in calculating the nonlinear polarization, it is necessary to solve Eqs. (3.19) self-consistently to all orders in $\tilde{\kappa}$ since it is quite possible for $\tilde{\kappa}L\sim1$ even if $U/kT\ll1$, as mentioned previously.

The polarization characteristics of the conjugate wave are quite interesting, especially if the pump-wave polarization vectors are orthogonal. For example, suppose the pump waves are linearly polarized in the $\hat{x}$ and $\hat{y}$ directions and the probe beam is right-circularly polarized. Then the conjugate wave will be left-circularly polarized. If the probe wave is linearly polarized at an angle θ with respect to one of the pump beams, the conjugate wave will be linearly polarized at an angle θ with respect to the other pump wave.

To completely determine the magnitude of the conjugate and probe waves at any point in the medium, we must specify the values of these fields at the end points, i.e., $z=0$ and L. The standard situation is[8] $E_p(0)=E_0$ and $E_c(L)=0$. For these conditions

$$E_p(z)=E_p(0)\frac{\cos[\kappa(z-L)]}{\cos(\kappa L)} , \tag{3.21a}$$

$$E_c(z)=-iE_p^*(0)\frac{\sin[\kappa(L-z)]}{\cos(\kappa L)} . \tag{3.21b}$$

Note that the probe wave is amplified and the magnitude of the conjugate wave can exceed E_0. Physically, one can understand this as follows. Via electrostrictive forces, a pump wave and the probe wave drive the microparticles into a spatial grating which scatters the other pump wave in such a manner as to form a conjugate wave. Similarly, the conjugate wave and one of the pump beams create a spatial grating which scatters the other pump wave into the probe wave. Thus, in particulate suspensions, the conjugate wave is generated and the probe wave is amplified by coherent scattering of laser radiation by electrostrictively generated spatial gratings.

The efficiency for generating conjugate waves is

$$\eta=\tan^2(\tilde{\kappa}L) \tag{3.22}$$

which can easily exceed unity. As a specific example, we consider a suspension of 1000-Å ZnSe spheres maintained in liquid N_2 at 80 K, irradiated by CO_2 laser radiation. If there are 1.6×10^{12} microspheres per cm^3, the extinction length due to Rayleigh scattering exceeds 60 cm and since neither ZnSe nor liquid N_2 absorb at 10.6 μm, there are no significant losses. If the polarization vectors of all the waves are parallel,

$$\tilde{\kappa}\simeq0.1I/T\ \text{cm}^{-1} , \tag{3.23}$$

where I is the laser intensity in W/cm^2 and the temperature is in kelvin. Thus, for an interaction length of 1 cm $\tilde{\kappa}L=1$ for a laser power of 0.8 kW/cm^2 at 80 K. This corresponds to an efficiency of 245%. Note that if the suspension is placed in a Fabry-Perot cavity with a cavity $Q=L_s/L\simeq100$ for the present case, pump powers on the order of 1 W/cm^2 will yield values of $\tilde{\kappa}L\simeq1$. The probe amplification ξ is given by

$$\xi=[\cos(\tilde{\kappa}L)]^{-2}=1+\eta . \tag{3.24}$$

If the polarization vectors of the pump waves are orthogonal and the probe wave is parallel to one beam, then, as noted above, the conjugate wave's polarization will be parallel to the second pump wave and $\tilde{\kappa}L\simeq0.071(I/T)$

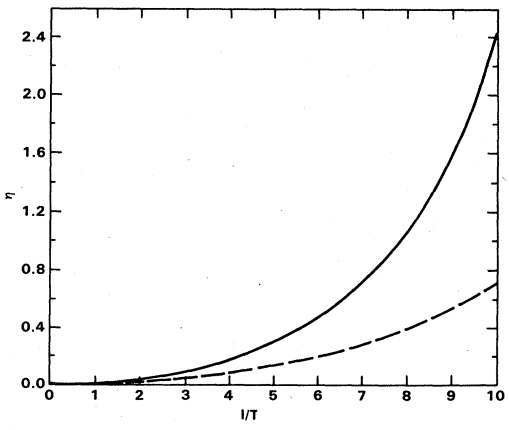

FIG. 2. Efficiency for the generation of conjugate waves in liquid suspensions of microspheres as a function of I/T for the cases in which the pump waves have parallel (solid) and orthogonal (dashed) polarizations. For the situation depicted, a density of 1.6×10^{12} cm^{-3} 1000-Å microparticles are irradiated by CO_2-laser radiation at 10.6 μm.

for the same parameters as Eq. (3.23). The phase conjugate efficiency for these two cases are depicted in Fig. 2 as a function of I/T.

Next, we consider the influence of scattering losses on phase conjugation in liquid suspensions of microspheres. In Appendix A, it is shown that the efficiency for generating conjugate waves is[22]

$$\eta=\frac{4\kappa^2 L_s^2 e^{-L/L_s}\tan^2(\kappa' L)}{[2\kappa' L_s+\tan(\kappa' L)]^2}\ , \tag{3.25}$$

where

$$\kappa'\equiv[\kappa^2 e^{-L/L_s}-(1/2L_s)^2]^{1/2} \tag{3.26}$$

which reduces to Eq. (3.22) in the limit that $L_s\to\infty$. Furthermore, the ratio of the probe intensity at the exit point to the initial intensity, i.e., ξ, is[22]

$$\xi=\frac{(2\kappa' L_s)^2}{[2\kappa' L_s\cos(\kappa' L)+\sin(\kappa' L)]^2} \tag{3.27}$$

which reduces to Eq. (3.24) in the limit $L_s\to\infty$. Figure 3 depicts the efficiency and probe amplification as a function of I/T for 1000-Å microspheres irradiated by a DF laser emitting on the 3.8-μm line. For the case depicted, the interaction length $L=\frac{1}{2}L_s$ with $L_s=2.91$ cm.

Finally, we consider the possibility of achieving oscillation in liquid suspensions of microspheres. In the limit that $L_s\to\infty$, this occurs whenever

$$\kappa L=(n+\tfrac{1}{2})\pi,\quad n=0,\pm1,\pm2,\ldots \tag{3.28}$$

i.e., both η and $\xi\to\infty$ as $\kappa L\to(n+\frac{1}{2})\pi$. Typical operating conditions for which one might hope to achieve gain for the medium described by Eq. (3.22) are $(IL/T)=5\pi$. For an interaction length of 1 cm with $T=80$ K, oscillation should occur for pump powers on the order of 1.256 kW/cm^2. This should be contrasted with atomic and molecular gases, e.g., CS_2, which typically requires hundreds of MW/cm^2 to achieve oscillation. Thus electrostrictive modulation of microparticles seems potentially to be far more efficient in generating conjugate waves than approaches based on virtual quantum transitions in atomic or molecular media.

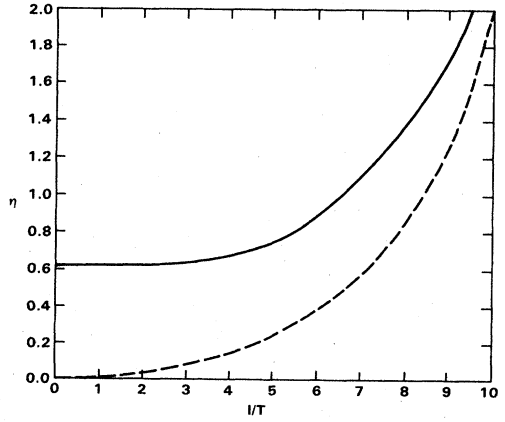

FIG. 3. Efficiency for the generation of conjugate waves (dashed) and amplification of the probe wave (solid) in liquid suspensions of microspheres as a function of I/T for the cases in which the pump waves have parallel polarizations. For the situation depicted, a density of 0.55×10^{12} cm^{-3} 1000-Å microparticles are irradiated by DF radiation at 3.8 μm.

IV. NON-STEADY-STATE CHARACTERISTICS

In this section we examine four-wave mixing in liquid suspensions of microspheres for certain non-steady-state conditions in the weak-field limit. Specifically, in (4.1), we examine the evolution to steady-state from the initial thermal equilibrium state of a uniform microparticle density for the case $\kappa L\ll1$. In (4.2), we study the situation in which $\kappa L\sim1$. For this case, the conjugate and probe fields interact with each other through the microparticles, and one must formulate the problem self-consistently.

A. Evolution to steady state in the small-signal regime

We are concerned with the transient behavior of the microparticle density in the small-signal regime as it evolves from the initial state

$$n=n_0 \tag{4.1a}$$

to the final state

$$n(\mathbf{r})=n_0\left[1-\frac{\overline{U(\mathbf{r})}}{kT}\right] \tag{4.1b}$$

and how this change is reflected in the nonlinear electrodynamics of the suspension.

The Nernst-Planck equation is

$$\frac{\partial n}{\partial t}=D\nabla^2 n-\frac{D}{kT}\nabla\cdot(\mathbf{F}n)\ . \tag{4.2}$$

In the small-signal regime, we may set

$$n(\mathbf{r},t)=n_0[1+p(\mathbf{r},t)]\ , \tag{4.3}$$

where $p(\mathbf{r},t)$ is of the order $U/kT\ll1$. Thus, in this limit

$$\frac{\partial p}{\partial t}=D\nabla^2 p+\left[\frac{D\alpha}{2kT}\right]\nabla^2\overline{E}^{\,2}(\mathbf{r},t)\ . \tag{4.4}$$

Next, we note that the components of the electrostrictive force that are of interest to us depend upon the magnitudes of both the probe and conjugate waves. Now, in the small-signal regime where

$$\kappa L\ll1\ ,$$

we can neglect intensity changes in the probe wave and ignore the presence of the conjugate wave. In that case, the source term on the right-hand side of Eq. (4.4) is independent of time and can readily be integrated. However, if $\kappa L\sim1$, there will be a significant increase of energy in the probe and conjugate waves and as a result, the electrostrictive force will vary in time. For this case, one must supplement Eq. (4.4) with equations which govern the time evolution of the probe and conjugate waves, i.e., the time-dependent analog of Eqs. (3.14). This shall be done in Sec. IV B.

As noted above, in the small-signal regime, we may ignore the conjugate wave and treat the pump and probe fields in the nondepleted wave approximation. To further simplify matters, we shall assume that $L_s \gg L$, so that we may ignore the effects of scattering losses. Next, we note that to first order in U/kT we may treat additively the various electrostrictive forces which give rise to a modulation of the microparticle density. Thus

$$p(\mathbf{r},t)=p_1(x,t)+p_2(y,t) , \tag{4.5}$$

where, as before, x and y are the coordinates along the $(\mathbf{K}-\mathbf{Q})$ and $(\mathbf{K}+\mathbf{Q})$ axes. Inserting Eq. (4.5) into Eq. (4.4), solving for $p_1(x,t)$ and $p_2(y,t)$, subject to the boundary condition $n(\mathbf{r}, t=0)=n_0$, we obtain

$$p_1(x,t)=2\pi\frac{\alpha\sqrt{I_1 I_p}}{ckT}\,|\hat{e}_1\cdot\hat{e}_p^*|\times(1-e^{-t/\tau_-})\cos\left[\frac{2\pi}{\Lambda_-}x+\phi_1\right] , \tag{4.6a}$$

$$p_2(y,t)=2\pi\frac{\alpha\sqrt{I_2 I_p}}{ckT}\,|\hat{e}_2\cdot\hat{e}_p^*|\times(1-e^{-t/\tau_+})\cos\left[\frac{2\pi}{\Lambda_+}y+\phi_2\right] , \tag{4.6b}$$

where

$$E_j E_p^*\cdot\hat{e}_p^*\equiv\frac{c}{4\pi}\,|\hat{e}_j\cdot\hat{e}_p^*|\sqrt{I_j I_p}\,e^{i\phi_j} . \tag{4.7}$$

Here, τ_+ (τ_-) is the diffusion time for microparticles to move a grating spacing in the x (y) directions:

$$\frac{1}{\tau_+}=\frac{4\pi^2 D}{\Lambda_+^2}\equiv\frac{2\pi}{3}\left[\frac{kT}{va\Lambda_+^2}\right] , \tag{4.8a}$$

$$\frac{1}{\tau_-}=\frac{4\pi^2 D}{\Lambda_-^2}\equiv\frac{2\pi}{3}\left[\frac{kT}{va\Lambda_-^2}\right] . \tag{4.8b}$$

Equations (4.6) describe the time evolution of the two spatial gratings from the initial condition of a uniform microparticle distribution. Note that the different polarization dependence, i.e., $|\hat{e}_1\cdot\hat{e}_p^*|$ and $|\hat{e}_2\cdot\hat{e}_p^*|$, enables one to examine the transient behavior of these two spatial gratings independently, especially if the polarization of the two pump beams are chosen to be orthogonal to each other. Typical values for $\tau_\pm$ vary from tens of seconds down to hundreds of microseconds, depending upon the microparticle size, host viscosity, grating spacing, and temperature. For example, for 1000-Å microspheres maintained in liquid Ar and irradiated by CO_2-laser light with probe and pump beams at 90°, we have

$$\tau_+=\tau_-\simeq 0.2\text{ s} ,$$

whereas for 200-Å microspheres irradiated with Nd:YAG (yttrium aluminum garnet) light at 1.06 μm in pressurized liquid N_2 at 100 K with $\nu\simeq 10^{-4}$ P

$$\tau_+=\tau_-\simeq 1\text{ ms} ,$$

with shorter times possible at higher pressures. Note that the grating arises from diffusion of the microparticles into particular spatial locations. This should be contrasted with the strong-field limit, to be discussed elsewhere, where the microparticles are driven into their positions by laser radiation.

There is another way to interpret Eqs. (4.6). Specifically, each spatial grating $p_1(x,t)$ and $p_2(y,t)$ can be interpreted as arising from two separate gratings which are out of phase with one another,

$$p_1(x,t)=p_1^{(1)}(x)-p_1^{(2)}(x,t) , \tag{4.9a}$$

where

$$p_1^{(1)}(x)\equiv 2\pi\frac{\alpha(I_1 I_p)^{1/2}}{ckT}\,|\hat{e}_1\cdot\hat{e}_p^*|\cos(2\pi x/\Lambda_-+\phi_1) , \tag{4.9b}$$

$$p_1^{(2)}(x,t)\equiv 2\pi\frac{\alpha(I_1 I_p)^{1/2}}{ckT}\times|\hat{e}_1\cdot\hat{e}_p^*|\,e^{-t/\tau}\cos(2\pi x/\Lambda_-+\phi_1) . \tag{4.9c}$$

Thus, the grating $p_1^{(2)}(x,t)$ is exactly out of phase with the first; however, as time proceeds, it gradually diffuses away, leaving only the first grating.

Next, we examine the transient behavior of the conjugate wave. The equation of motion for the conjugate wave

$$\left[\frac{\partial}{\partial z}+\frac{1}{v}\frac{\partial}{\partial t}\right]\epsilon_c(z,t)=i\kappa_+(1-e^{-t/\tau_+})\epsilon_p^*+i\kappa_-(1-e^{-t/\tau_-})\epsilon_p^* , \tag{4.10a}$$

$$\left[\frac{\partial}{\partial z}-\frac{1}{v}\frac{\partial}{\partial t}\right]\epsilon_p(z,t)=i\kappa_+(1-e^{-t/\tau_+})\epsilon_c^*+i\kappa_-(1-e^{-t/\tau_-})\epsilon_c^* , \tag{4.10b}$$

where

$$\kappa_+=n_0\alpha(\omega)Q\frac{\alpha(\omega)E_1E_2}{2kT}\,|\hat{e}_1\cdot\hat{e}_p^*| , \tag{4.11a}$$

$$\kappa_-=n_0\alpha(\omega)Q\frac{\alpha(\omega)E_1E_2}{2kT}\,|\hat{e}_2\cdot\hat{e}_p^*| . \tag{4.11b}$$

In the small-signal regime, ϵ_p^* is treated as a constant and Eq. (4.10b) is ignored. The solution to Eq. (4.10a) is then

$$\epsilon_c(z,t)=-iE_p\kappa_+ v\tau_+\left[\left[\frac{L-z}{v\tau_+}\right]-e^{-t/\tau_+}(1-e^{-(L-z)/v\tau_+})\right]-iE_p\kappa_- v\tau_-\left[\left[\frac{L-z}{v\tau_-}\right]-e^{-t/\tau_-}(1-e^{-(L-z)/v\tau_-})\right] . \tag{4.12}$$

In general, $L-z \ll v\tau_{\pm}$ because $v \sim 3\times 10^{10}$ cm/s, $\tau_{\pm} \sim 10^{-6}$–10^{2} s and $L-z \sim 1$–10 cm $\ll v\tau_{\pm}$. Thus, we may expand Eq. (4.12) in powers of $(L-z)/v\tau_{\pm}$ to obtain

$$\epsilon_c(z,t) = iE_p\kappa_+(L-z)(1-e^{-t/\tau_+}) - iE_p\kappa_-(L-z)(1-e^{-t/\tau_-}) . \quad (4.13)$$

By neglecting higher-order terms in Eq. (4.12), we are ignoring effects arising from the finite travel time of electromagnetic waves through the conjugating medium. Since $\tau_{\pm} \gg L/v$, it is clear that the nonlinear medium will respond to the presence of the probe field only long after the incident radiation has traversed the medium. This lag, which characterizes all artificial dielectrics, arises from the fact that it takes the microparticles much longer to traverse a spatial grating distance than for light to propagate through the entire medium. This should be contrasted with conjugation processes based on virtual quantum transitions, which may occur instantaneously on a time scale set by L/v.

The time evolution of the efficiency $\eta(t)$ is given by

$$\eta(t) = (\kappa_+ L)^2(1-e^{-t/\tau_+})^2 + (\kappa_- L)^2(1-e^{-t/\tau_-})^2 \quad (4.14)$$

which for $\theta = \pi/2$ reduces to

$$\eta(t) = (\kappa L)^2[1-e^{-t/\tau}]^2 , \quad (4.15a)$$

where $\tau_+ = \tau_- \equiv \tau$. Furthermore, the growth of the probe wave is

$$\xi(t) = 1 + (\kappa L)^2(1-e^{-t/\tau})^2 . \quad (4.15b)$$

Note that Eqs. (4.14) and (4.15) are valid only for times $t \gg L/v$.

Figure 4 depicts the efficiency versus t/τ for the generation of conjugate waves for $\kappa L = 0.1$. An examination of this figure reveals that for $t/\tau \ll 1$, $\eta(t) \sim (t/\tau)^2$ in accord with Eq. (4.16). The efficiency approaches its steady-state value of 1% when $t \sim 5\tau$. Finally, Fig. 5 depicts the spacetime dependence of $\delta n(x,t)$. Specifically, the spatial variation of δn is plotted over a grating spacing, i.e., $0 \le x \le \Lambda$ for the times $t/\tau = 0$, 0.1, 0.5, 1.0, 5.0, and 10. An examination of this figure reveals that microparticles reach steady state in a time 5τ.

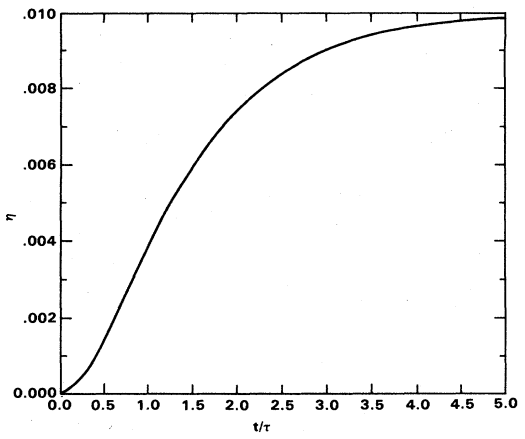

FIG. 4. Efficiency for the generation of conjugate waves as a function of t/τ for the case $\kappa L = 0.1$ and $\theta = \pi/2$.

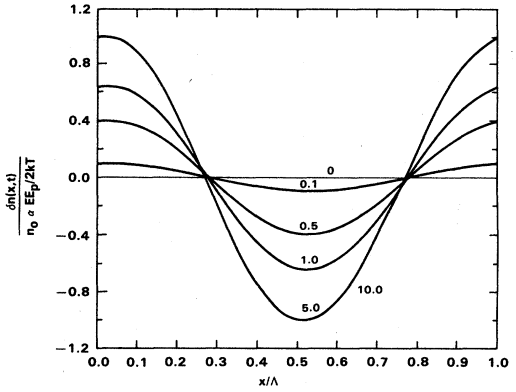

FIG. 5. Time evolution of the normalized spatial dependence of the microparticle distribution $\delta n(x,t)/(n_0\alpha EE_p/2kT)$ over a grating spacing for the case depicted in Fig. 4.

B. Evolution to steady state in the large-signal regime

In this section, we examine the transient behavior of the microspheres, as well as the probe and conjugate waves in the large-signal regime, where $\kappa L \sim 1$. In this regime, there is a significant exchange of energy between the various electromagnetic waves so that the entire system, microparticles, conjugate and probe radiation, must be treated self-consistently. However, since

$$U/kT \ll 1 ,$$

the electrostrictive forces are still sufficiently weak that only a small fraction of the microspheres are involved in phase conjugation and no saturation effects should appear in the microparticle density.

We first note that, due to the long time lag of the microparticle response to electromagnetic waves, the nonlinear polarization $P_{\rm NL}(\mathbf{r},t)$ is nonlocal in time. In particular, if $n(\mathbf{r},t) = n_0 p(\mathbf{r},t)$, then $p(\mathbf{r},t)$ obeys

$$\left[\frac{\partial}{\partial t} - D\nabla^2\right] p(\mathbf{r},t) = D\frac{\alpha(\omega)}{2\kappa T} \sum_{\substack{i,j \\ i\neq j}}{}' \epsilon_1^*(\mathbf{r},t)\epsilon_j(\mathbf{r},t)(\hat{e}_i^* \cdot \hat{e}_j)(\mathbf{k}_i - \mathbf{k}_j)^2 e^{i(\mathbf{k}_i - \mathbf{k}_j)\cdot\mathbf{r}} . \quad (4.16)$$

The prime in Eq. (4.16) implies that no terms involving only the pump waves enter into the sum. Since the time dependence of both the conjugate and probe waves is unknown, one can only formally integrate Eq. (4.16), resulting in a nonlocal expression for the nonlinear polarization.

We can readily avoid these difficulties by using Laplace transform techniques, similar to the approach taken by Rigrod *et al.*[11] Thus, writing

$$p(\mathbf{r},t) = [f_+(\mathbf{r},t)e^{i(\mathbf{K}+\mathbf{Q})\cdot\mathbf{r}} + f_-(\mathbf{r},t)e^{-i(\mathbf{K}-\mathbf{Q})\cdot\mathbf{r}}] + \text{c.c.} \quad (4.17)$$

we have, for pump waves of equal magnitude

$$\left[\frac{\partial}{\partial t}+\frac{1}{\tau_{\pm}}\right]f_{\pm}(\mathbf{r},t)=\frac{\alpha(\omega)E}{2kT\tau_{\pm}}[\epsilon_c(\mathbf{r},t)+\epsilon_p^*(\mathbf{r},t)]\ . \tag{4.18}$$

In Eq. (4.18) we have ignored the effect of the spatial dependence of the field amplitudes on the diffusion process. As this is of order $\kappa\Lambda_{\pm}\ll 1$, this approximation should give rise to negligible errors.

If we allow for the time dependence of the complex amplitudes, the equations for $\epsilon_c(\mathbf{r},t)$ and $\epsilon_p^*(\mathbf{r},t)$ become

$$\left[\frac{\partial}{\partial z}+\frac{1}{v}\frac{\partial}{\partial t}\right]\epsilon_c(z,t)=in_0E[f_+(z,t)+f_-(z,t)]\ , \tag{4.19a}$$

$$\left[-\frac{\partial}{\partial z}+\frac{1}{v}\frac{\partial}{\partial t}\right]\epsilon_p^*(z,t)=-in_0E[f_+(z,t)+f_-(z,t)]\ . \tag{4.19b}$$

Equations (4.18) and (4.19) describe the transient behavior of the conjugate and probe waves in the nondepleted pump approximation for situations in which

$$\frac{\partial}{\partial z}\epsilon_j\ll k\epsilon_j\quad(j=p,c)\ , \tag{4.20a}$$

$$\frac{\partial}{\partial t}\epsilon_j\ll\omega\epsilon_j\quad(j=p,c)\ . \tag{4.20b}$$

Taking the Laplace transform of Eq. (4.18), we have

$$\tilde{f}_{\pm}(z,s)=\left[\frac{\alpha(\omega)E/2kT}{s\tau_{\pm}+1}\right][\tilde{\epsilon}_c(z,s)+\tilde{\epsilon}_p^*(z,s)]\ , \tag{4.21}$$

where $\tilde{A}(z,s)$ denotes the Laplace transform of $A(z,t)$. An examination of Eq. (4.21) reveals that only low-frequency components of $f_{\pm}(z,s)$, i.e., those which satisfy

$$s\le 1/\tau_{\pm}\ , \tag{4.22}$$

will contribute significantly to the formation of a spatial grating. Inserting Eq. (4.21) into the Laplace transform of Eq. (4.19) yields

$$\left[\frac{\partial}{\partial z}+\frac{s}{v}\right]\tilde{\epsilon}_c(z,s)=\left[\frac{i\kappa_+}{1+s\tau_+}+\frac{i\kappa_-}{1+s\tau_-}\right][\tilde{\epsilon}_c(z,s)+\tilde{\epsilon}_p^*(z,s)]-\frac{1}{v}\epsilon_c(z,0)\ , \tag{4.23a}$$

$$\left[\frac{\partial}{\partial z}-\frac{s}{v}\right]\epsilon_p^*(z,s)=\left[\frac{i\kappa_+}{1+s\tau_+}+\frac{i\kappa_-}{1+s\tau_-}\right][\tilde{\epsilon}_c(z,s)+\tilde{\epsilon}_p^*(z,s)]-\frac{1}{v}\epsilon_p^*(z,0)\ . \tag{4.23b}$$

Next, we simplify Eqs. (4.23) by recalling that due to the diffusive character of the transient response of the microspheres, only the low-frequency components of the nonlinear polarization are significant. Hence, we may neglect the term $(s/v)\tilde{\epsilon}_j$ or by extension $(1/v)(\partial/\partial t)\epsilon_j$ in the Maxwell equations, since

$$\frac{\partial}{\partial z}\tilde{\epsilon}_j(z,s)\sim k\tilde{\epsilon}_j(z,s)\gg\frac{s}{v}\tilde{\epsilon}_j(z,s)\sim\frac{1}{v\tau}\tilde{\epsilon}_j(z,s)\ .$$

We can further simplify matters by restricting ourselves to the case of equal grating spacing, i.e., $\theta=\pi/2$. If the probe wave is switched on at $t=0$, then we show in Appendix B that

$$\tilde{\epsilon}_c(z,t)=\frac{-iE_p}{2\pi i}\int_{\gamma-i\infty}^{\gamma+i\infty}\frac{ds}{s}e^{st}\frac{\sin[\kappa(L-1)/(1+s\tau)]}{\cos[\kappa L/(1+s\tau)]}\times\exp\left[-i\frac{\kappa z}{1+s\tau}\right] \tag{4.24a}$$

and

$$\epsilon_p^*(z,t)=\frac{E_p}{2\pi i}\int_{\gamma-i\infty}^{\gamma+i\infty}\frac{ds}{s}e^{st}\frac{\cos[\kappa(L-z)/(1+s\tau)]}{\cos[\kappa L/(1+s\tau)]}\times\exp\left[-i\frac{\kappa z}{1+s\tau}\right]\ . \tag{4.24b}$$

An examination of Eqs. (4.24) reveals that there are poles at

$$s=0\ , \tag{4.25a}$$

$$s_n=\frac{1}{\tau}\left[-1+\frac{\kappa L}{(n+\frac{1}{2})\pi}\right],\quad n=0,\pm1,\pm2,\ldots\ . \tag{4.25b}$$

The pole at $s=0$ arises from suddenly switching on the probe field, whereas the ones at $s=s_n$ arise from the dynamics of phase conjugation. The dynamic poles asymptotically approach $-1/\tau$ and appear at discrete points along the interval

$$-\left[1+\frac{\kappa L}{\pi/2}\right]\le s_n\tau\le-\left[1-\frac{\kappa L}{\pi/2}\right]\ . \tag{4.26}$$

Note that so long as $\kappa L<\pi/2$, all of the singularities lie to the left of $s=0^+$. If $\kappa L>\pi/2$, then at least one of these poles lies to the right of $s=0^+$ and the system is

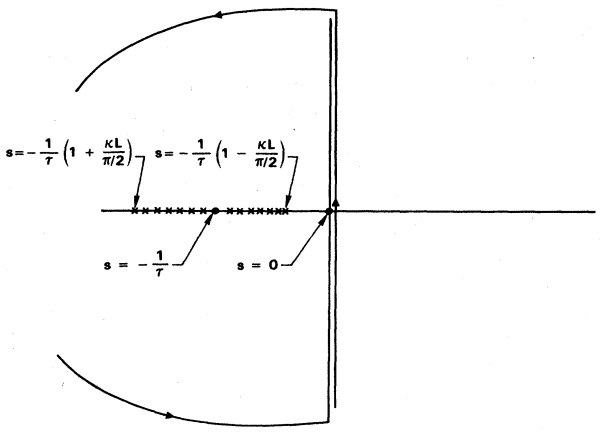

FIG. 6. Bromwich contour in the complex s plane.

unstable in the sense that the wave grows exponentially in time (at least in the nondepleted pump approximation). Closing the Bromwich contour in the left-hand-side s plane,[23] as depicted in Fig. 6, and noting that the residues A_n of $[\cos(\kappa L/1+s_n\tau)]^{-1}$ are

$$A_n=\frac{(-1)^n\kappa L}{[(n+\frac{1}{2})\pi]^2\tau} \tag{4.27}$$

we have

$$\epsilon_c(z,t)=iE_p\left[\frac{\sin[\kappa(L-z)]}{\cos(\kappa L)}e^{-i\kappa z}-\kappa Le^{-t/\tau}\sum_{n=-\infty}^{\infty}\frac{\exp[\kappa L(t/\tau)/(n+\frac{1}{2})\pi-i(n+\frac{1}{2})\pi z/L]}{[(N+\frac{1}{2}\pi]^2[1-\kappa L/(n+\frac{1}{2})\pi]}\cos[(n+\frac{1}{2})\pi z/L]\right], \tag{4.28a}$$

$$\epsilon_p^*(z,t)=E_p\left[\frac{\cos[L(L-z)]}{\cos(\kappa L)}e^{-i\kappa z}-\kappa Le^{-t/\tau}\sum_{n=-\infty}^{\infty}\frac{\exp[\kappa L(t/\tau)/(n+\frac{1}{2})\pi-i(n+\frac{1}{2})\pi z/L]}{[(n+\frac{1}{2}\pi]^2[1-\kappa L/(n+\frac{1}{2})\pi]}\sin[(n+\frac{1}{2})\pi z/L]\right]. \tag{4.28b}$$

Finally, the efficiency for generating conjugate waves is

$$\eta(t)=\left[\tan(kL)-e^{-t/\tau}\sum_{n=-\infty}^{\infty}\frac{\exp\{[\kappa L/(n+\frac{1}{2})\pi](t/\tau)\}}{[(n+\frac{1}{2})\pi]^2-\kappa L(n+\frac{1}{2}\pi]}\kappa L\right]^2 \tag{4.29a}$$

whereas the amplification of the pump wave is

$$\xi(t)=1+\eta^2(t)\,. \tag{4.29b}$$

An examination of Eqs. (4.29) reveals that they reduce to their corresponding values in small-signal regime when $\kappa L\ll 1$. Furthermore, if $t\ll\tau$

$$\eta(t)\to\left[\frac{\kappa L}{4}(t/\tau)\right]^2, \tag{4.30a}$$

$$\xi(t)\to 1+\left[\left[\frac{\kappa L}{4}\right]\left[\frac{t}{\tau}\right]\right]^2, \tag{4.30b}$$

as is demonstrated in Appendix B. Next, we consider the behavior of the probe and conjugate waves in the limit $t\gg\tau$. Then, if $\kappa L<\pi/2$, the leading terms are

$$\eta(t)\to\left\{\tan(\kappa L)+\frac{\kappa L}{(\pi/2)^2(1-2\kappa L/\pi)}\times\exp\left[-\left[1-\frac{\kappa L}{\pi/2}\right]\frac{t}{\tau}\right]\right\}^2, \tag{4.31a}$$

$$\xi(t)\to 1+\left[\tan(\kappa L)+\frac{\kappa L}{(\pi/2)^2}\times\frac{\exp[-(1-2\kappa L/\pi)t/\tau]}{(1-2\kappa L/\pi)}\right]^2. \tag{4.31b}$$

Equations (4.31) assert that the probe and conjugate waves achieve their steady-state values on a time scale set by

$$\tau_R=\frac{\tau}{(1-2\kappa L/\pi)} \tag{4.32}$$

so that the larger the nonlinear mixing parameter, the longer it takes for the medium to achieve steady state (provided electrostrictive forces are still sufficiently weak that $U\ll kT$). Furthermore, as $\kappa L\to\pi/2$ from below,

$$\eta(t)\to\left[\frac{1}{(\pi/2)(1-2\kappa L/\pi)}\right]^2\times\left\{1+\left[\frac{\kappa L}{\pi/2}\right]\exp\left[-\left[1-\frac{\kappa L}{\pi/2}\right]\frac{t}{\tau}\right]\right\}^2, \tag{4.33a}$$

$$\xi(t)\to 1+\left[\frac{1}{(\pi/2)(1-2\kappa L/\pi)}\right]^2\times\left\{1+\frac{\kappa L}{\pi/2}\exp\left[-\left[1-\frac{\kappa L}{\pi/2}\right]\frac{t}{\tau}\right]\right\}^2 \tag{4.33b}$$

so that the probe and conjugate waves become very intense and the time to achieve steady state $\tau_R\gg\tau$. Note that these equations are unstable in the sense that they do not achieve steady state in the limit that κL exceeds $\pi/2$. Instead, the probe and conjugate waves grow exponentially without bound. This difficulty arises from and reflects the fact that we have neglected saturation effects in our treatment of phase conjugation for these media. Specifically, we have restricted ourselves to the nondepleted pump approximation and, in addition, have included only terms of order (U/kT) in determining the influence of electrostrictive forces on the microparticle density. Hence, our results are valid only if $\delta n\ll n_0$. However, if

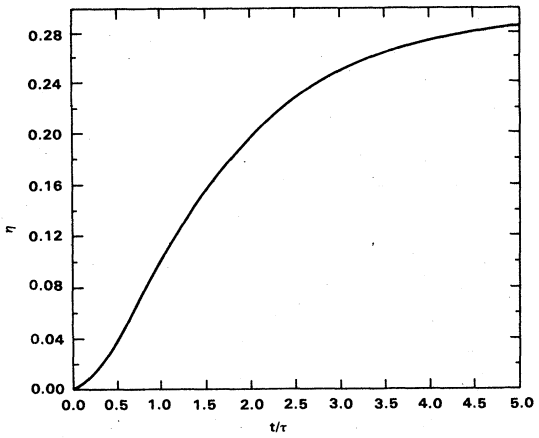

FIG. 7. Time evolution of the efficiency for the case $\kappa L = \frac{1}{2}$.

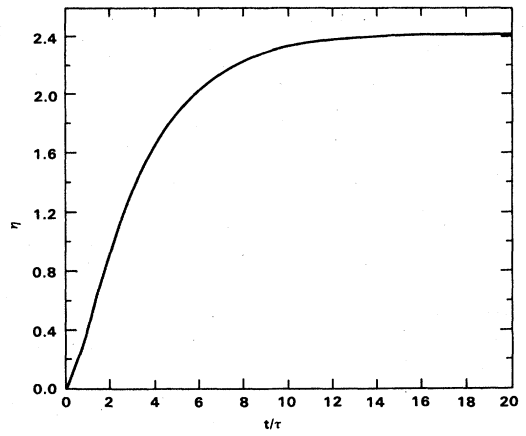

FIG. 8. Time evolution of the efficiency for the case $\kappa L = 1$.

the conjugate and probe waves grow too large, this will be no longer be the case, and Eqs. (4.29) are no longer valid.

Figure 7 depicts the time evolution of the efficiency for the case $\kappa L = \frac{1}{2}$. Here, the response time $\tau_R = 1.47\tau$ and η achieves a steady-state value of 29.8%. An examination of this figure reveals that the efficiency varies as $(t/\tau)^2$ for $t \ll \tau$ and approaches its steady-state value exponentially for $t \gg \tau$, in accord with Eqs. (4.30) and (4.31).

Figure 8 depicts the time evolution of the efficiency for $\kappa L = 1$. Here, the response time $\tau_R = 2.75\tau$ so that steady state is not achieved until a time $\tau \sim 8\tau$. The overall behavior of the efficiency for this case is similar to that depicted in Fig. 7, except that it takes longer to achieve steady state and the efficiency is generally larger at any given time.

Next, we focus our attention on the behavior of the microparticle distribution. Thus, combining Eqs. (4.17), (4.21), and (4.24), we have

$$\delta n(x,t) = \frac{\alpha(\omega) E E_p}{2kT} n_0 \,\mathrm{Re}\left[\exp\left[\frac{2\pi i x}{\Lambda}\right] \int_{\lambda - i\infty}^{\lambda + i\infty} \frac{ds}{2\pi i} \frac{\exp(st)}{s\tau(1+s\tau)} \left[1 - i\tan\frac{\kappa L}{1+s\tau}\right]\right] . \tag{4.34}$$

The first term in the intergrand of Eq. (4.34) is just the small-signal result and represents the response of the microparticle density to the initial probe wave. The second term arises from the presence of the conjugate wave. Note that this term is $3\pi/2$ out of phase with respect to the first term. This implies that the spatial grating pattern impressed on the microparticles will not be in phase with the probe wave due to the presence of the conjugate wave. Furthermore, since the conjugate wave is growing in time, the spatial distribution itself will shift in the sense that the position of the zeros and nodes of $\delta n(x,t)$ will change in time.

In Appendix C we evaluate the integral in Eq. (4.34) and find

$$\delta n(x,t) = \tfrac{1}{2} n_0 \frac{\alpha E E_p}{kT} \times \{ (1 - e^{-t/\tau}) \cos(2\pi x/\Lambda) + [\eta^{1/2}(t) + \lambda(t)] \sin(2\pi x/\Lambda) \} , \tag{4.35}$$

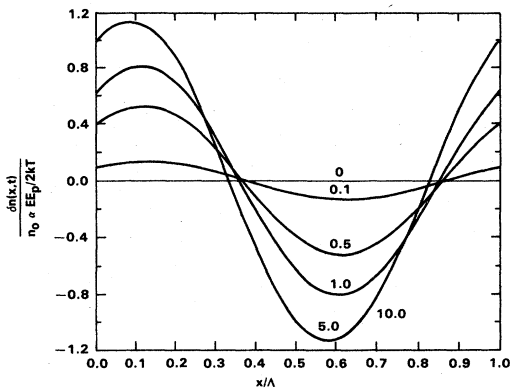

FIG. 9. Time evolution of the normalized spatial dependence of the microparticle distribution $\delta n(x,t)/(n_0 \alpha E E_p/2kT)$ over a grating spacing for the case $\kappa L = \frac{1}{2}$.

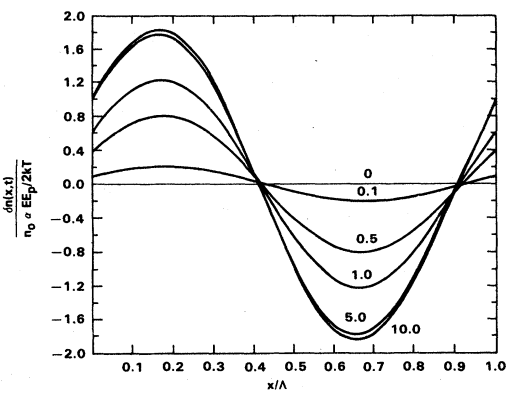

FIG. 10. Time evolution of the normalized spatial dependence of the microparticle distribution $\delta n(x,t)/(n_0 \alpha E E_p/2kT)$ over a grating spacing for the case $\kappa L = 1$.

where $\lambda(t)$ is a well-behaved function which is specified in Appendix C. The first term in Eq. (4.35) is the linear response of the microparticle to the probe wave, whereas the second represents further adjustments of the microparticle distribution due to the presence of the conjugate wave, as well as amplification of the probe wave. Note that if $\kappa L \ll 1$, Eq. (4.35) reduces to the small-signal regime, i.e., Eqs. (4.9). Furthermore, for $t \ll \tau$

$$\delta n(x,t) \rightarrow \tfrac{1}{2} n_0 \frac{\alpha E E_p}{kT} \frac{t}{\tau} \cos(2\pi x/\Lambda) , \tag{4.36}$$

i.e., the microparticles are initially in phase with the probe field since the conjugate wave has not had sufficient time to influence matters. For $t \gg \tau$,

$$\delta n(x,t) \rightarrow \tfrac{1}{2} n_0 \frac{E E_p(L)}{kT} \cos(2\pi x/\Lambda - \kappa L) , \tag{4.37}$$

where $E_p(L)$ is the amplitude of the probe wave as it exits the medium.

Figure 9 depicts the behavior of $\delta n(x,t)$ over one spatial grating distance for the case $\kappa L = \frac{1}{2}$. Note the change in positions of the zeros and nodes at different times. Note too that steady state is reached on the same time scale as the probe and conjugate waves, as expected, since they will adiabatically follow the microparticle distribution. Finally, Fig. 10 depicts $\delta n(x,t)$ for the case $\kappa L = 1$.

V. DISCUSSION AND CONCLUSIONS

In this paper, we have examined degenerate four-wave mixing in liquid suspensions of microspheres which are operating in the diffusive limit. For these media, electrostrictive forces modulate the microparticle density in such a way that two spatial gratings, which are orthogonal to each other, are created. Phase conjugate waves are generated via coherent scattering of pump radiation off of these two gratings. For these media, the four-wave-mixing coefficient tends to be fairly large with a broad, nonresonant bandwidth, provided the radiation does not lie within an absorption band of the suspension. In addition, the response times for these media are relatively slow. These properties, in turn, arise from and reflect the manner in which the microparticle gratings are set up, as well as their interaction with electromagnetic radiation. To underscore the physical content of this research, we contrast degenerate four-wave mixing in electrostrictive media to media in which such processes are achieved via virtual quantum transitions, e.g., typical atomic or molecular gases.

We first recall degenerate four-wave mixing in typical gases, e.g., CS_2 or Na vapor. In such media, the phase of the transition electric dipole moment of the atom or molecule is controlled by the incident laser radiation via virtual quantum processes, as discussed in Ref. 2. The time scale for this process to be achieved is on the order of the Rabi flopping time, which is typically on the order of nanoseconds down to picoseconds, depending upon laser power and system. The spatial gratings which give rise to the generation of conjugate waves consist of an ordered collection of phased dipoles, the particular ordering being determined by the incident radiation. The time scale for this to occur is just the sum of the transit time of light plus the Rabi flopping time. If the interaction length is 1 cm, the transit time for a typical gas will be 33 ps. Thus, typical response times for generating conjugate waves in atomic or molecular gases will vary from tens of picoseconds to nanoseconds. Note that the formation of these gratings does not involve the motion of the individual atoms or molecules, but rather occurs via a particular ordering of the phases of the atomic wave functions. This should be contrasted to liquid suspensions of microspheres in which the spatial gratings are set up by electrostrictive modulation of the microparticle density. As discussed extensively in Sec. IV, the temporal response for these systems is dominated by the dynamics of the particulate motion which in the limit treated here is diffusive. Since the time it takes to reorder the phase of an atomic wave function is much less than the time required for a microparticle to diffuse a grating spacing, it immediately follows that the response time for processes based on virtual quantum transitions is much shorter than those involving motion based on electrostrictive forces.

The frequency dependence of the four-wave-mixing coefficient also sharply delineates the fundamental differences between suspensions and gases. In suspensions, electrostrictive forces, as well as the nonlinear polarizability, arise from coherent scattering processes which set up the spatial grating, generate the conjugate wave and amplify the probe wave. For such processes, the radiation frequency enters into the problem via the microparticle's polarizability. In particular, if the radiation wavelength is large compared to the microparticle dimensions, the frequency will enter into the four-wave-mixing coefficient only through the dielectric constants of the constituents. Thus, so long as we are in the Rayleigh regime and not too close to an absorption band of these constituents, the nonlinear mixing coefficients for suspensions should depend only weakly on frequency. In contrast, media which generate conjugate waves via virtual quantum transitions will exhibit a sharp frequency dependence. This feature arises from the fact that virtual processes give rise to energy denominators in nonlinear optical susceptibilities which are strongly dependent on frequency. Furthermore, atomic media may exhibit two-photon resonances which greatly enhance the size of the nonlinear susceptibility for degenerate four-wave mixing. However, such processes do not occur in electrostrictive media and, in fact, as noted in Sec. III, make no contribution to κ.

Next we contrast the size of the nonlinear susceptibilities associated with degenerate four-wave mixing for electrostrictive and atomic processes. For electrostrictive processes,

$$\chi^{(3)}_{\text{micro}} \sim \frac{\alpha^2}{kT} \sim \frac{a^6}{kT} ,$$

whereas for an atom

$$\chi^{(3)}_{\text{atom}} \sim \frac{p^4}{(\hbar\Omega)^3} ,$$

where p is the transition electric dipole moment and Ω the difference in the laser and transition frequency. Typically, $p \sim e a_0$ and for nonresonant situations $\hbar\Omega \sim e^2/a_0$,

where a_0 is the Bohr radius and e the electric charge. Hence,

$$\chi^{(3)}_{\text{atom}} \sim \frac{a_0^6}{e^2/a_0} .$$

Since $a \gg a_0$ and $kT \ll e^2/a_0$, it is easy to see why $\chi^{(3)}_{\text{micro}} \gg \chi^{(3)}_{\text{atom}}$. Table I summarizes the above discussion.

Next we comment on the range of parameters for the suspension to remain in the diffusive regime. As noted in Sec. IV, the grating formation time is the time required for a microparticle to diffuse a grating spacing, i.e.,

$$\tau_D^{-1} = \frac{2\pi}{3}\left[\frac{kT}{\nu a \Lambda^2}\right] . \tag{5.1}$$

If, instead, the microparticle's dynamics are governed entirely by the electromagnetic forces, then Smith *et al.* have shown[15]

$$\tau_F^{-1} = \frac{4\alpha E E_p}{3a\nu\Lambda^2} . \tag{5.2}$$

Clearly, the suspension will be in the diffusive regime if $\tau_D \ll \tau_F$, or

$$\frac{\alpha E E_p}{kT} \ll 1 . \tag{5.3}$$

In turn, Eq. (5.3) implies that only a small fraction of the microparticles be involved in phase conjugation, i.e., $\delta n \ll n_0$ and, therefore, that there are no saturation effects. We note that the observations of Smith *et al.*[15] were in the regime where $U \geq kT$, so that no direct comparisons appear possible.

Another interesting feature of liquid suspensions in the diffusive regime is that the time to achieve steady state increases with κL, as discussed in Sec. IV. In particular, if $\kappa L < \pi/2$, the diffusion time τ is replaced by

$$\tau \rightarrow \tau_R = \frac{\tau}{1 - 2\kappa L/\pi} . \tag{5.4}$$

The physical content of Eq. (5.4) is the following: The probe wave initially sets up a grating which coherently scatters the pump radiation to generate a conjugate wave. However, since κL is fairly large, the resultant conjugate wave will be of the same order of magnitude as the probe field. Consequently, it will, in turn, interact with the microparticles to modify the spatial grating. Since the conjugate wave is $3\pi/2$ out of phase with the probe wave, there will be some readjustment of the microparticle distribution which will increase the time it takes to attain steady state.

APPENDIX A: INFLUENCE OF RAYLEIGH SCATTERING ON PHASE CONJUGATION

In this appendix we examine the influence of Rayleigh scattering on phase conjugation and derive Eqs. (3.25) and (3.27). We begin by noting that due to Rayleigh scattering, the pump amplitudes are functions of position, and following Yariv and Pepper,[22] we have

$$E_1(z) = \epsilon_1(0)\exp(-\alpha z/2) , \tag{A1a}$$

$$E_2(z) = \epsilon_2(L)\exp[-\alpha(L-z)/2] \tag{A1b}$$

so that $E_1(z)E_2(z)$ is independent of z. The relevant equations are

$$\hat{\mathcal{O}}_+ \epsilon_c^{(1)}(z) = i\kappa\epsilon_p^{(1)*}(z) + i\kappa[\sigma_+(z)\epsilon_c^{(1)}(z) + \sigma_-(z)\epsilon_c^{(2)}(z)] , \tag{A2a}$$

$$\hat{\mathcal{O}}_+ \epsilon_c^{(2)}(z) = -i\kappa\epsilon_p^{(2)*}(z) + i\kappa[\sigma_-(z)\epsilon_c^{(1)}(z) + \sigma_+(z)\epsilon_c^{(2)}(z)] , \tag{A2b}$$

$$\hat{\mathcal{O}}_- \epsilon_p^{(1)}(z) = u\kappa\epsilon_c^{(1)*}(z) + i\kappa[\sigma_+(z)\epsilon_p^{(1)}(z) + \sigma_-(z)\epsilon_p^{(2)}(z)] , \tag{A2c}$$

$$\hat{\mathcal{O}}_- \epsilon_p^{(2)}(z) = -i\kappa\epsilon_c^{(2)*}(z) + i\kappa[\sigma_-(z)\epsilon_p^{(1)}(z) + \sigma_+(z)\epsilon_p^{(2)}(z)] , \tag{A2d}$$

TABLE I. Comparison of degenerate four-wave mixing in liquid suspensions to an atomic vapor.

Property	Suspension of microspheres	Atomic gas
Mechanism for the generation of conjugate waves	Electrostrictive modulation of the microparticle density	Electromagnetic ordering of the phases of the atomic wave functions
Response time	Diffusive Λ^2/D	Rabi flopping time $\hbar/p\epsilon$
Nonlinear susceptibility (per particle)	$\frac{a^6}{kT}$	$\frac{a_0^6}{e^2/a_0}$ (nonresonant)
Resonance behavior	None	Strong
Frequency dependence of κ	Broadband, provided no significant absorption occurs	Narrow

where the superscripts refer to the components of the conjugate and probe waves along the $\hat{a}_1$ and $\hat{a}_2$ directions. Furthermore, the quantities $\hat{\mathcal{O}}_{\pm}$ and $\sigma_{\pm}$ are defined by

$$\hat{\mathcal{O}}_{\pm}=\pm\frac{d}{dz}+\frac{1}{\alpha L_s}\ , \tag{A3a}$$

$$\sigma_{\pm}=\frac{E_1^2(z)\pm E_2^2(z)}{\epsilon_1(0)\epsilon_2(L)}\ . \tag{A3b}$$

The terms involving $\sigma_{\pm}(z)$ can be treated in a fashion similar to the approach used in Eqs. (3.24) with κ replaced by

$$\kappa\rightarrow\kappa\int^z dz'\,\sigma_+(z') \tag{A4}$$

in the phase factors. Although the $\sigma_-(z)$ terms give rise to a coupling between the two different polarizations, it does not affect the properties of the conjugate wave, except for a phase term:

$$E_p(z)=E_0\frac{2\kappa L_s\cos[\kappa'(L-z)]+\sin[\kappa'(L-z)]}{2\kappa' L_s\cos(\kappa' L)+\sin(\kappa' L)}\ , \tag{A5a}$$

$$E_c(z)=-iE_0e^{-L/2L_s}\frac{2\kappa L_s\sin[\kappa'(L-z)]}{2\kappa' L\cos(\kappa' L)+\sin(\kappa' L)}\ . \tag{A5b}$$

APPENDIX B: PROPERTIES OF THE PROBE AND CONJUGATE WAVES IN THE STRONG-SIGNAL REGIME

The relevant equations are

$$\frac{\partial}{\partial z}\tilde{\epsilon}_c(z,s)=\frac{i\kappa}{1+s\tau}[\tilde{\epsilon}_c(z,s)+\tilde{\epsilon}_p^*(z,s)]\ , \tag{B1a}$$

$$\frac{\partial}{\partial z}\tilde{\epsilon}_p^*(z,s)=\frac{i\kappa}{1+s\tau}[\tilde{\epsilon}_c(z,s)+\tilde{\epsilon}_p^*(z,s)]\ . \tag{B1b}$$

Defining $\tilde{G}_c(z,s)$ and $G_p^*(z,s)$ by

$$\tilde{\epsilon}_p(z,s)=\tilde{G}_c(z,s)\exp\left[-\frac{i\kappa}{1+s\tau}z\right]\ , \tag{B2a}$$

$$\tilde{\epsilon}_p^*(z,s)=\tilde{G}_p^*(z,s)\exp\left[-\frac{i\kappa}{1+s\tau}z\right]\ , \tag{B2b}$$

we have

$$\frac{\partial}{\partial z}\tilde{G}_c(z,s)=\frac{i\kappa}{1+s\tau}G_p^*(z,s)\ , \tag{B3a}$$

$$\frac{\partial}{\partial z}\tilde{G}_p(z,s)=\frac{i\kappa}{1+s\tau}\tilde{G}_c(z,s)\ . \tag{B3b}$$

Solving Eqs. (4.26) for $\tilde{G}_c(z,s)$ and $\tilde{G}_p^*(z,s)$, using Eq. (B3) yields

$$\tilde{\epsilon}_c(z,s)=-i\frac{\sin[\kappa(L-z)/(1+s\tau)]}{\cos[\kappa L/(1+s\tau)]}e^{-i\kappa z/(1+s\tau)}\epsilon_p^*(0,s)\ , \tag{B4a}$$

$$\tilde{\epsilon}_p^*(z,s)=\frac{\cos[\kappa(L-z)/(1+s\tau)]}{\cos[\kappa L/(1+s\tau)]}e^{-i\kappa z/(1+s\tau)}\epsilon_p^*(0,s)\ , \tag{B4b}$$

which satisfies the appropriate boundary conditions at $z=0$ and L. To make further progress, it is necessary to carry out the inverse Laplace transform of Eqs. (B4). In particular

$$\epsilon_c(z,t)=-\frac{i}{\sqrt{2\pi}}\int_{\gamma-i\infty}^{\gamma+i\infty}ds\,e^{st}\tilde{\epsilon}_c(z,s)\ , \tag{B5a}$$

$$\epsilon_p^*(z,t)=-\frac{i}{\sqrt{2\pi}}\int_{\gamma-i\infty}^{\gamma+i\infty}ds\,e^{st}\tilde{\epsilon}_p^*(z,s)\ , \tag{B5b}$$

where γ lies to the right of the poles of $\tilde{\epsilon}_c(z,s)$ and $\tilde{\epsilon}_p^*(z,s)$.

Next, we derive Eqs. (4.30) by noting that for $t/\tau\ll 1$, the efficiency can be written as

$$\eta(t)=\left[\tan(\kappa L)-\sum_{n=-\infty}^{\infty}\frac{\kappa L}{[(n+\frac{1}{2})\pi]^2[1-\kappa L/(n+\frac{1}{2})\pi]}+\frac{t}{\tau}\sum_{n=-\infty}^{\infty}\frac{\kappa L}{[(n+\frac{1}{2})\pi]^2}\right]^2\ . \tag{B6}$$

Now,[24]

$$\tan\left[\frac{\pi x}{4}\right]=\sum_{n=1}^{\infty}\frac{x}{(2n-1)^2(x/2)^2} \tag{B7a}$$

and

$$\frac{\pi}{4}=\sum_{n=1}^{\infty}\frac{1}{(2n-1)^2}\ . \tag{B7b}$$

Inserting Eqs. (B7) into Eq. (B6) yields Eq. (4.30).

APPENDIX C: TIME EVOLUTION OF THE MICROPARTICLE DISTRIBUTIONS

In this appendix, we derive Eq. (4.35). Rewriting the integral in Eq. (4.34) as

$$I(t)=\lim_{\tau'\rightarrow\tau}\left[\int_{\gamma-i\infty}^{\gamma+i\infty}\frac{ds}{2\pi i}\frac{\exp(st)}{s\tau(1+s\tau)}\times\left[1-i\tan\frac{\kappa L}{1+s\tau'}\right]\right] \tag{C1}$$

we have poles at $s=0$, $-1/\tau$, and $-(1/\tau')[1+\kappa L/(n+\frac{1}{2})\pi]$. Carrying out the integral yields

$$I(t)=(i-e^{-t/\tau})-i[\eta^{1/2}(t)+\lambda(t)]\ , \tag{C2}$$

where

$$\lambda(t)\equiv\lim_{\tau'\rightarrow\tau}\left[\tan\left[\frac{\kappa L}{\tau-\tau'}\right]-\sum_{n=-\infty}^{\infty}\frac{\kappa L\exp\{[\kappa L/(n+\frac{1}{2})\pi](t/\tau)\}}{[(n+\frac{1}{2})\pi]^2\{1-[\kappa L/(\tau-\tau')]/(n+\frac{1}{2})\pi\}}\right]e^{-t/\tau}\ . \tag{C3}$$

The function $\lambda(t)$ vanishes in the limits $t\rightarrow 0$ and $t\rightarrow 10$ and is convergent everywhere. Inserting Eq. (C2) into Eq. (4.34) yields Eq. (4.35).

[1]R. A. Fisher and B. J. Feldman in *1980 McGraw-Hill Yearbook of Science and Technology* (McGraw-Hill, New York, 1980).
[2]C. R. Guiliano, Phys. Today **34** (No. 4), 27 (1981).
[3]*Optical Phase Conjugation,* edited by R. A. Fisher (Academic, New York, 1983).
[4]R. L. Abrams and R. C. Lind, Opt. Lett. **2**, 94 (1978).
[5]A. Elci, D. Rogovin, D. Depatie, and D. Harrison, J. Opt. Soc. Am. **70**, 990 (1980).
[6]G. Rivoire, J. L. Ferrier, J. Grazengel, and Phu Xuan, J. Phys. (Paris) Colloq. **44**, C2-81 (1983).
[7]R. K. Jain and H. B. Klein in Ref. 3.
[8]A. Yariv and D. M. Pepper, Opt. Lett. **1**, 16 (1978).
[9]P. Avizonis, F. A. Hopf, W. D. Bomberger, S. F. Jacobs, A. Tomita, and K. H. Womack, Appl. Phys. Lett. **31**, 435 (1977).
[10]B. Ya. Zeldovich, V. I. Popovicheo, V. V. Ragul'skii, and F. S. Faizullov, Sov. Phys.—JETP **15**, 109 (1972).
[11]W. W. Rigrod, R. D. Fisher, and B. J. Feldman, Opt. Lett. **5**, 105 (1980).
[12]A. Yariv, Opt. Commun. **21**, 49 (1977).
[13]M. D. Levenson, Opt. Lett. **5**, 182 (1980).
[14]D. M. Pepper, D. Fekete, and A. Yariv, Opt. Lett. **3**, 7 (1978).
[15]P. W. Smith, A. Ashkin, and W. J. Tomilson, Opt. Lett. **6**, 294 (1981).
[16]A. J. Palmer, Opt. Lett. **5**, 54 (1980).
[17]J. P. Gordon, Phys. Rev. A **8**, 14 (1973).
[18]S. O. Sari and D. Rogovin, Opt. Lett. **9**, 414 (1984).
[19]S. Chandrasekhar, Rev. Mod. Phys. **15**, 1 (1943).
[20]E. M. Lifshitz and O. P. Pitaevskii, *Physical Kinetics* (Pergamon, New York, 1981).
[21]L. M. Landau and E. M. Lifshitz, in *Electrodynamics of Continuous Media* (Pergamon, New York, 1960).
[22]D. M. Pepper and A. Yariv, in Ref. 3.
[23]H. W. Wyld, *Mathematical Methods for Physics* (Benjamin, Reading, Mass., 1976).
[24]I. S. Gradshteyn and I. M. Ryzhik, *Tables of Integrals, Series and Products* (Academic, New York, 1965).